



OPEN ACCESS

EDITED BY

Linkai Huang,
Sichuan Agricultural University,
China

REVIEWED BY

Min Sun,
Sichuan Agricultural University,
China
Mingshu Cao,
AgResearch Ltd.,
New Zealand

*CORRESPONDENCE

Yong Ding
dingyong@caas.cn

[†]These authors have contributed equally to this work and share first authorship

SPECIALTY SECTION

This article was submitted to
Plant Breeding,
a section of the journal
Frontiers in Plant Science

RECEIVED 15 July 2022

ACCEPTED 26 August 2022

PUBLISHED 04 October 2022

CITATION

Wan D, Wan Y, Zhang T, Wang R and
Ding Y (2022) Multi-omics analysis reveals
the molecular changes accompanying
heavy-grazing-induced dwarfing of *Stipa
grandis*.
Front. Plant Sci. 13:995074.
doi: 10.3389/fpls.2022.995074

COPYRIGHT

© 2022 Wan, Wan, Zhang, Wang and Ding.
This is an open-access article distributed
under the terms of the [Creative Commons
Attribution License \(CC BY\)](https://creativecommons.org/licenses/by/4.0/). The use,
distribution or reproduction in other
forums is permitted, provided the original
author(s) and the copyright owner(s) are
credited and that the original publication in
this journal is cited, in accordance with
accepted academic practice. No use,
distribution or reproduction is permitted
which does not comply with these terms.

Multi-omics analysis reveals the molecular changes accompanying heavy-grazing-induced dwarfing of *Stipa grandis*

Dongli Wan^{1†}, Yongqing Wan^{2†}, Tongrui Zhang¹,
Ruigang Wang² and Yong Ding^{1*}

¹Institute of Grassland Research, Chinese Academy of Agricultural Sciences, Hohhot, China,
²College of Life Sciences, Inner Mongolia Agricultural University, Hohhot, China

Heavy grazing significantly reduces *Stipa grandis* growth. To enhance our understanding of plant responses to heavy grazing, we conducted transcriptomic, proteomic, and metabolic analyses of the leaves of non-grazed plants (NG) and heavy-grazing-induced dwarf plants (HG) of *S. grandis*. A total of 101 metabolites, 167 proteins, and 1,268 genes differed in abundance between the HG and NG groups. Analysis of Kyoto Encyclopedia of Genes and Genomes pathways among differentially accumulated metabolites (DAMs) revealed that the most enriched pathways were flavone and flavonol biosynthesis, tryptophan metabolism, and phenylpropanoid biosynthesis. An integrative analysis of differentially expressed genes (DEGs) and proteins, and DAMs in these three pathways was performed. Heavy-grazing-induced dwarfism decreased the accumulation of DAMs enriched in phenylpropanoid biosynthesis, among which four DAMs were associated with lignin biosynthesis. In contrast, all DAMs enriched in flavone and flavonol biosynthesis and tryptophan metabolism showed increased accumulation in HG compared with NG plants. Among the DAMs enriched in tryptophan metabolism, three were involved in tryptophan-dependent IAA biosynthesis. Some of the DEGs and proteins enriched in these pathways showed different expression trends. The results indicated that these pathways play important roles in the regulation of growth and grazing-associated stress adaptations of *S. grandis*. This study enriches the knowledge of the mechanism of heavy-grazing-induced growth inhibition of *S. grandis* and provides valuable information for restoration of the productivity in degraded grassland.

KEYWORDS

Stipa grandis, heavy grazing, transcriptomic, proteomic, metabolic

Introduction

Stipa grandis (Poaceae, $2n=44$) is a wind-pollinated C_3 perennial bunchgrass that flowers in mid- to late-July and the seeds ripen in late August or early September (Zhao et al., 2008; Wu et al., 2010b). The mature plants form dense tussocks that are approximately 30 cm high with long and thin leaves (Zhao et al., 2008). *S. grandis* is among the dominant

plant species in typical steppe of the Inner Mongolian Plateau (Wu et al., 2010b). *S. grandis*-dominated grassland, the most common and representative community in the Eurasian steppe (Gao et al., 2018b), has been degraded to varying degrees (Xiao et al., 1995; Wu et al., 2010a), which greatly affects grassland productivity.

Overgrazing and climate change (such as aridification) are the main factors responsible for degradation of grassland of the Inner Mongolian Plateau (Gao et al., 2018a). Livestock grazing is a major anthropogenic disturbance of grasslands on a global scale (Zhao et al., 2009). To respond to grazing, plants alter their morphological and functional traits (Zhao et al., 2009). For instance, the individual plant height and biomass (of leaves, stems, and the whole plant) of *Leymus chinensis* are significantly restricted under overgrazing (Li et al., 2015). The size of individual *S. grandis* plants is minimized to cope with frequent grazing or overgrazing (Wan et al., 2015; Li et al., 2018). The leaf photosynthetic activity, as indicated by net photosynthetic rate, stomatal conductance, intercellular carbon dioxide concentration, and transpiration rate, is markedly decreased following overgrazing (Ren et al., 2017). In recent years, several studies have been conducted to explore the molecular mechanism of plant dwarfism resulting from overgrazing at the transcription and protein levels (Wan et al., 2015; Ren et al., 2018a,b). However, little information is available on the protein and metabolic mechanisms responsible for the response of *S. grandis* to overgrazing.

Proteins are macromolecular compounds that function as the biochemical units in all cellular processes (Mann et al., 2013). Proteomics is the large-scale study of proteins and is crucial for understanding biological processes at the molecular level (Pandey and Mann, 2000; Zhang et al., 2014). Proteomics is widely used to study the processes of plant development and stress responses (Chen et al., 2015; Liu et al., 2015; Jiang et al., 2019; Zhan et al., 2019; Li et al., 2020; Lv et al., 2021), and provides essential tools to study global protein expression and dissect the unique functions underlying the many plant-specific biological processes (Job et al., 2011).

Plant metabolites, which are essential for humans as a nutritional source, play vital roles in the interaction of plants and the surrounding environment (Chen et al., 2020). It has been estimated that 200,000 to 1,000,000 metabolites exist in the plant kingdom (Saito and Matsuda, 2010). Metabolomics, which is the analysis of almost all metabolites in a biological sample using qualitative and quantitative methods, acts as a bridge to link the genome and phenome (Shi et al., 2020). Metabolomic approaches have been used to study metabolism in plant developmental processes and responses to environmental stimuli, such as low temperature (Yang et al., 2019b), salt (Li and Song, 2019), high light (Zhang et al., 2019), fruit development and ripening (Xu et al., 2020), and color variation (Yang et al., 2019a; Li et al., 2021b). Combined analysis of omics data has become a powerful tool to explain diverse developmental processes, environmental responses, and regulatory mechanisms (Chen et al., 2021; Guo et al., 2021; Xu et al., 2021; Li et al., 2021a; Qin et al., 2022). For instance, comparative transcriptomic and metabolomic analysis

revealed an abscisic acid-dependent acclimation mechanism to drought and cold stress in maize (Guo et al., 2021). Combined transcriptomic, proteomic, and metabolomic analyses revealed that core metabolic processes were influenced in seeds of transgenic maize engineered for enhanced carotenoid synthesis (Decourcelle et al., 2015). Multi-omics analysis has highlighted distinct roles of central carbon metabolism to assist high productivity of specialized metabolites in glandular trichomes of tomato (Balcke et al., 2017), uncovered sequential roles associated with abscisic acid during seed maturation (Chauffour et al., 2019), and provided new insights into the decline in fruit quality of apple grown under high nitrogen fertilization (Wang et al., 2021b).

In this study, we performed transcriptomic, tandem mass tag (TMT) label-based proteomic, and widely targeted metabolic profiling in leaves of *S. grandis* grown under non-grazing and heavy-grazing treatments. The important metabolic pathways involved in the grazing response were evaluated by combined analysis of the omics data. The aim of this study was to elucidate the mechanism by which heavy grazing depresses *S. grandis* growth from different molecular aspects. The results will improve our understanding of the impact of grazing on metabolite and protein accumulation in *S. grandis*, and provide valuable information for restoration of productivity in degraded grassland.

Materials and methods

Study area and sampling

Sampling was conducted at the Inner Mongolia Typical Grassland Ecological Protection and Restoration Research Station of the Chinese Academy of Agricultural Sciences, located in Xilinhot, Inner Mongolia, China (116°32'E, 44°15'N), on August 2, 2018. The study region has a temperate semiarid continental climate, with a mean annual temperature of 0.7°C, and lowest and highest temperatures of -41.1°C in January and 38.5°C in August, respectively (Liu et al., 2019). The mean annual precipitation is 300–360 mm with maximum precipitation in the period from June to August (Zhang et al., 2020). The dominant plant species in the study area comprised *S. grandis* and *L. chinensis*.

Grazing had been prohibited from the study area from 2007 to 2013, and the grazing experiments were conducted since 2014. The non-grazed (NG) plot was continually protected from grazing from 2014 to 2018. The heavy-grazing (HG) plot was grazed from 2014 to 2017 by 12 sheep. Grazing started in the middle of June and ended in the middle of September each year. The NG and HG plots were 1.33 Ha in area. The grazing pressure of HG is 1.4 standard sheep unit per hectare per year (SSU·ha⁻¹·y⁻¹), which is apparently higher than that of locally allowed standards (0.84 SSU·ha⁻¹·y⁻¹). Each grazing treatment was established with three replicate plots. In 2018, prior to grazing, half of each HG plot was fenced to exclude grazing disturbance, and the individuals of *S. grandis* in this area retained a dwarf phenotype compared with the plants in the NG area (Supplementary Figure S1); the HG samples for subsequent analysis

were collected from plants growing in the exclusion area. The leaves from three bunches of *S. grandis*, sampled at a vigorous growth stage from one plot for each treatment, were respectively pooled as one biological replicate, immediately frozen in liquid nitrogen, and stored at -80°C for subsequent total RNA, protein, and metabolite extraction. Three biological replicates were taken from one sampling plot for each treatment.

Transcriptome analysis

Total RNA of each sample was isolated from leaves of three bunches of *S. grandis* using TRIzol Reagent. The RNA integrity was examined using agarose gel electrophoresis and an Agilent 2,100 Bioanalyzer. The RNA concentration and purity were determined with a NanoDrop spectrophotometer based on the $\text{OD}_{260}/\text{OD}_{280}$ and $\text{OD}_{260}/\text{OD}_{230}$ ratios, respectively.

For cDNA library construction, mRNAs were enriched from the total RNAs using Oligo (dT) magnetic beads, after fragmentation into short segments using fragmentation buffer, used as templates to synthesize the first-strand cDNA with random hexamer primers and reverse transcriptase. Following second-strand cDNA synthesis, the fragments were end-repaired, a single adenine nucleotide was added to the 3' end, and then ligated with sequencing adapters. Subsequently, the cDNA fragments were selected and PCR amplification was performed to obtain the final cDNA library. In total, six libraries were sequenced using an Illumina NovaSeq 6,000 platform.

Following processing for quality control, transcriptome assembly was performed with Trinity (Grabherr et al., 2011). Gene functions were annotated using the Kyoto Encyclopedia of Genes and Genomes (KEGG),¹ Gene Ontology (GO),² National Center for Biotechnology Information (NCBI) non-redundant (NR),³ Swiss-Prot,⁴ UniProtKB/TrEMBL,⁵ and Clusters of Orthologous Groups of proteins (COG/KOG)⁶ databases. The transcript levels of unigenes were calculated using the fragments per kilobase per million fragments (FPKM) method. Differential expression analysis between the HG and NG treatments was performed using DESeq2 (Love et al., 2014; Varet et al., 2016). The significantly differentially expressed genes (DEGs) were determined with the thresholds of $|\log_2(\text{HG}/\text{NG})| \geq 1$ and $\text{FDR} \leq 0.05$. Analyses of GO term and KEGG pathway enrichment of the DEGs were conducted with the R version 3.5.1 software using R package “clusterProfiler” (Yu et al., 2012) using the threshold of a corrected value of $p \leq 0.05$ to determine significant enrichment.

1 <http://www.genome.jp/kegg/>

2 www.geneontology.org

3 <http://www.ncbi.nlm.nih.gov>

4 <http://www.expasy.ch/sprot>

5 <https://www.uniprot.org/uniprotkb?facets=reviewed%3Afalse&query=%2A>

6 <https://www.ncbi.nlm.nih.gov/COG/>

Proteome analysis

Protein extraction and TMT labeling

Protein extraction from leaves of each sample for proteomic analysis was performed following a previously described method (Wang et al., 2021a). The protein concentration was calculated using the Bradford assay with bovine serum albumin as the standard (Bradford, 1976). Protein quality was examined using SDS-PAGE. The proteins extracted from each sample were digested with Trypsin Gold (Promega, Madison, WI, United States) at 37°C for 16 h. The peptide was desalted using a C18 cartridge and dried by vacuum centrifugation. The TMT labeling of peptides was performed using TMTsixplex reagents (TMTsixplex™ Isobaric Label Reagent Set, Thermo Fisher, Waltham, MA, United States) in accordance with the manufacturer's instructions.

HPLC fractionation and LC–MS/MS analysis

Fractionation of the TMT-labeled peptide mix was performed on a Rigol L3000 HPLC using a C18 column ($4.6\text{ mm} \times 250\text{ mm}$, $5\text{ }\mu\text{m}$), with a column temperature of 50°C . Mobile phases A and B were water solutions containing 2% and 98% acetonitrile (pH 10.0), respectively. The TMT-labeled peptide mix was dissolved in 1 ml A and the supernatant was used as the injection sample. The peptides were separated into 15 fractions based on the following elution gradient: 3% B, 5 min; 3–8% B, 0.1 min; 8–18% B, 11.9 min; 18–32% B, 11 min; 32–45% B, 7 min; 45–80% B, 3 min; 80% B, 5 min; 80%–5% B, 0.1 min; and 5% B, 6.9 min. Following drying under vacuum, the samples were reconstituted in 0.1% (v/v) formic acid (FA) in water and used for LC–MS/MS analyses.

For proteomic analyses, the EASY-nLC™ 1200 UHPLC system (Thermo Fisher) was employed to analyze the samples. A Q Exactive™ HF-X Orbitrap mass spectrometer (Thermo Fisher) was used to obtain the peptides in the data-dependent acquisition (DDA) mode. Briefly, $2\text{ }\mu\text{g}$ peptides were dissolved in 0.1% FA and injected into a C18 Nano-Trap column ($2\text{ cm} \times 100\text{ }\mu\text{m}$, $5\text{ }\mu\text{m}$). The peptides were separated with a ReproSil-Pur 120 C18-AQ analytical column ($15\text{ cm} \times 150\text{ }\mu\text{m}$, $1.9\text{ }\mu\text{m}$), with a linear gradient from 5% to 100% eluent B (0.1% FA in 80% acetonitrile) in eluent A (0.1% FA in H_2O) for 90 min with a flow rate of 600 nl/min.

For DDA, the MS conditions were set as follows: spray voltage 2.3 kV, capillary temperature 320°C , range of full MS scans 350–1,500 m/z , resolution 60,000 (200 m/z), automatic gain control (AGC) target value 3×10^6 , and maximum ion injection time 20 ms. Based on the full MS scan, the 40 most abundant precursor ions were selected for higher-energy collisional dissociation fragment analysis. Resolution was set to 15,000, with AGC target value 1×10^5 , maximum ion injection time 45 ms, normalized collision energy of peptide fragmentation 32%, intensity threshold 8.3×10^3 , and dynamic exclusion parameter 60 s.

Protein identification and bioinformatics analysis

For protein identification, Proteome Discoverer (version 2.2) was used to search the raw data derived from MS analysis against the *S. grandis* transcriptome database (NCBI Sequence Read Archive database: PRJNA867365). The reporter quantification type was set as TMTsixplex. Trypsin was specified as an enzyme with a maximum of two missed cleavage sites. Mass tolerance for precursor and fragment was 10 ppm and 0.02 Da, respectively. Dynamic modifications were set as oxidation of methionine and TMTsixplex labeling lysine. The fixed modification was set as carbamidomethyl on cysteine. The parameters used for N-terminal modifications were acetylation of peptide N-terminus and TMTsixplex labeling N-terminus. Peptides were quantified according to the peak areas of corresponding mass reporters. The sequence of the peptides was determined by the mass-to-charge ratio of the peptide fragment ion peak. To reduce the frequency of false positives, the searched data were subsequently filtered through Proteome Discoverer. A peptide–spectrum match of 95% confidence was identified as credible, and the proteins containing at least one unique peptide were identified as credible. The false discovery rate (FDR) value was set at <5%.

Protein annotation was conducted using the GO, KEGG, and COG databases. For TMT quantification of proteins, the fold change (FC) between HG and NG samples was determined from the mean ratios of the TMT reporter ion intensities in the MS/MS spectra (m/z 126, 127–130C, 131) from all raw data sets. The significance of the differences was calculated using the corresponding value of p of each protein in two compared samples determined using Student's t -test. The thresholds of $FC \geq 1.2$ or $FC \leq 0.83$ and value of $p \leq 0.05$ were applied to detect differentially expressed proteins (DEPs). The functional subgroups and metabolic pathway enrichment for the DEPs were determined using the GO and KEGG databases.

Metabolite extraction and profiling

Metabolite extraction and profiling of the HG and NG samples was conducted by Wuhan Metware Biotechnology Co., Ltd. (Wuhan, China). Metabolite extraction, metabolite data acquisition, and assessment followed standard protocols as described in full previously (Chen et al., 2013; Li et al., 2021a). Briefly, the freeze-dried leaves were ground to powder using a mixer mill (MM 400, Retsch) with a zirconia bead (30 Hz, 1.5 min). One hundred milligram powder was extracted with 1.0 ml 70% aqueous methanol overnight at 4°C. After centrifugation (10,000g, 10 min), the supernatant was filtrated using a micropore filter membrane (0.22 μ m pore size) for LC–MS analysis. A LC–ESI–MS/MS system (UPLC, Shim-pack UFLC SHIMADZU CBM30A system, Kyoto, Japan; MS, Applied Biosystems 6,500 QTRAP, Framingham, MA, USA) was used for the UPLC–MS analysis. The chromatographic conditions were as follows: column, Waters ACQUITY UPLC HSS T3 C18 (1.8 μ m, 2.1 mm \times 100 mm); solvent

system, water (0.04% acetic acid), acetonitrile (0.04% acetic acid); elution gradient, water: acetonitrile was 95:5 (V/V) at 0 min, 5:95 (V/V) at 11.0 and 12.0 min, 95:5 (V/V) at 12.1 and 15.0 min; flow rate 0.4 ml min⁻¹; column temperature 40°C, sample injection volume 2 μ l. The mass spectrometry conditions: ESI temperature 500°C; ion spray voltage 5,500 V, curtain gas 25 psi; collision-activated dissociation was set to high. Instrument tuning was performed with 10 μ mol/l polypropylene glycol solutions in triple quadrupole mode, and mass calibration was performed with 100 μ mol/l polypropylene glycol solutions in linear ion trap mode. Metabolite identification was performed using the MWDB database.⁷ Quantitative metabolite analysis was conducted using the multiple reaction monitoring mode (Fraga et al., 2010).

Pearson's correlation analysis was used to analyze the correlation among samples within a group to assess biological repeatability. Hierarchical cluster analysis was conducted with R software⁸ to determine the metabolite accumulation patterns among different samples. Unsupervised principal component analysis (PCA) was employed to analyze the variability between the HG and NG groups as well as the three replications in each group.

The metabolite FC was calculated as the ratio of the mean metabolite abundance of HG plants relative to NG plants. The differentially accumulated metabolites (DAMs) were determined by a combination of the FC values and variable influence on projection (VIP) values. Partial least squares–discriminant analysis (PLS-DA), which is a supervised multivariate method, was used to maximize the metabolome differences between a pair of samples. The VIP value was used to check the relative importance of each metabolite in the PLS-DA model. Metabolites with $VIP \geq 1$ and $FC \geq 2$ or $FC \leq 0.5$ were identified as significantly differentially accumulated. The KEGG database was accessed for metabolite classification and pathway enrichment analysis.

Weighted correlation network analysis

Co-expression networks of DAMs and genes were constructed with R version 3.5.1 software using the weighted gene co-expression network analysis (WGCNA) package (version 1.69), the parameter were set as follow: powerEstimate 18, mergeCutHeight 0.25, and minModuleSize 50.

Results

Transcriptome profile of *Stipa grandis*

To investigate the molecular basis of the impact of heavy grazing on *S. grandis*, transcriptome profiling was performed and the transcript abundances were compared between the HG and

⁷ <http://www.metwarebio.com/list/27.html>

⁸ <https://www.r-project.org/>

NG samples (Supplementary Table S1). In total, 1,268 DEGs were detected, of which 860 were up-regulated and 408 were down-regulated (Figure 1A; Supplementary Table S2). Seventy-two GO terms were significantly enriched among the DEGs (Supplementary Figure S2). The most enriched KEGG pathways among these DEGs were the ribosome, plant–pathogen interaction, limonene and pinene degradation, lysine biosynthesis, ascorbate and aldarate metabolism, stilbenoid, diarylheptanoid, and gingerol biosynthesis; and histidine metabolism pathways (Figure 1B). The ribosome and plant–pathogen interaction pathways were significantly enriched ($p \leq 0.05$; Figure 1B).

TMT label-based proteome profile of *Stipa grandis*

The proteomic differences between the HG and NG groups were analyzed using TMT-based LC–MS/MS. Detailed information on the quality control is presented in Supplementary Figure S3. In total, 7,456 proteins were detected, of which 7,392 were annotated with functional terms from at least one of the GO, KEGG, and COG databases (Figure 2A; Supplementary Table S3). The coefficient of variation for most proteins was less than 20% (Figure 2B), which demonstrated high repeatability among the three biological replicates in each HG and NG group.

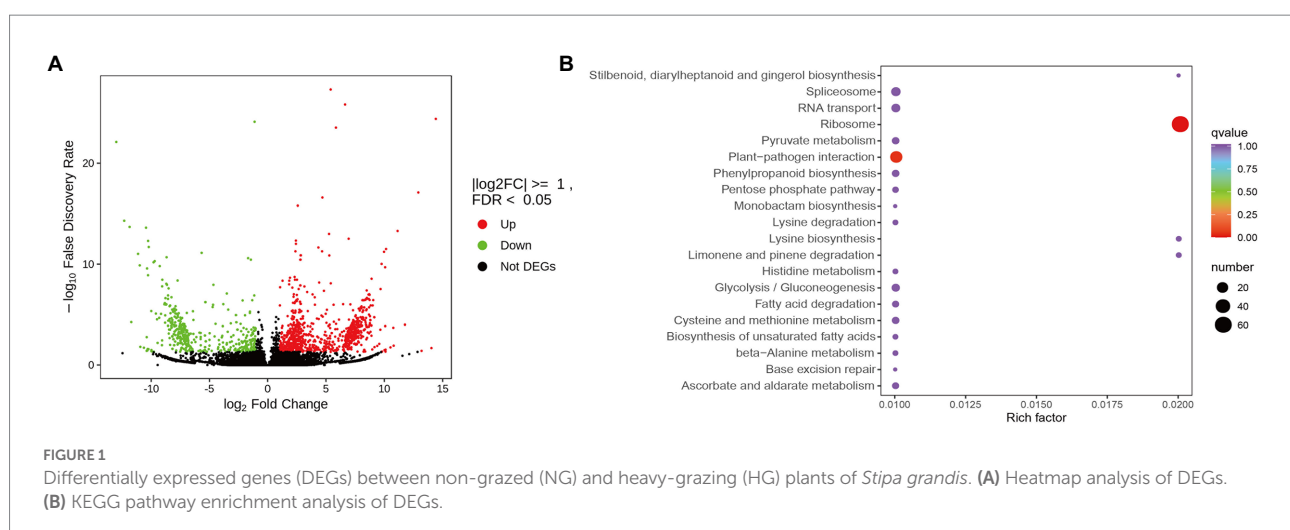
The abundance of 167 proteins differed significantly between the HG and NG groups with the thresholds $FC \geq 1.2$ or $FC \leq 0.83$, and value of $p \leq 0.05$. The expression of 135 DEPs was upregulated, whereas that of 32 DEPs was downregulated, in HG compared with NG (Figure 2C). Functional enrichment analysis showed that the DEPs were significantly enriched with 28 GO terms ($p \leq 0.05$, Figure 2D; Supplementary Table S4). The five most enriched terms in the molecular function category were catalase activity, peroxidase activity, heme binding, oxidoreductase activity, and D-aminoacyl-tRNA deacylase activity. The five most enriched

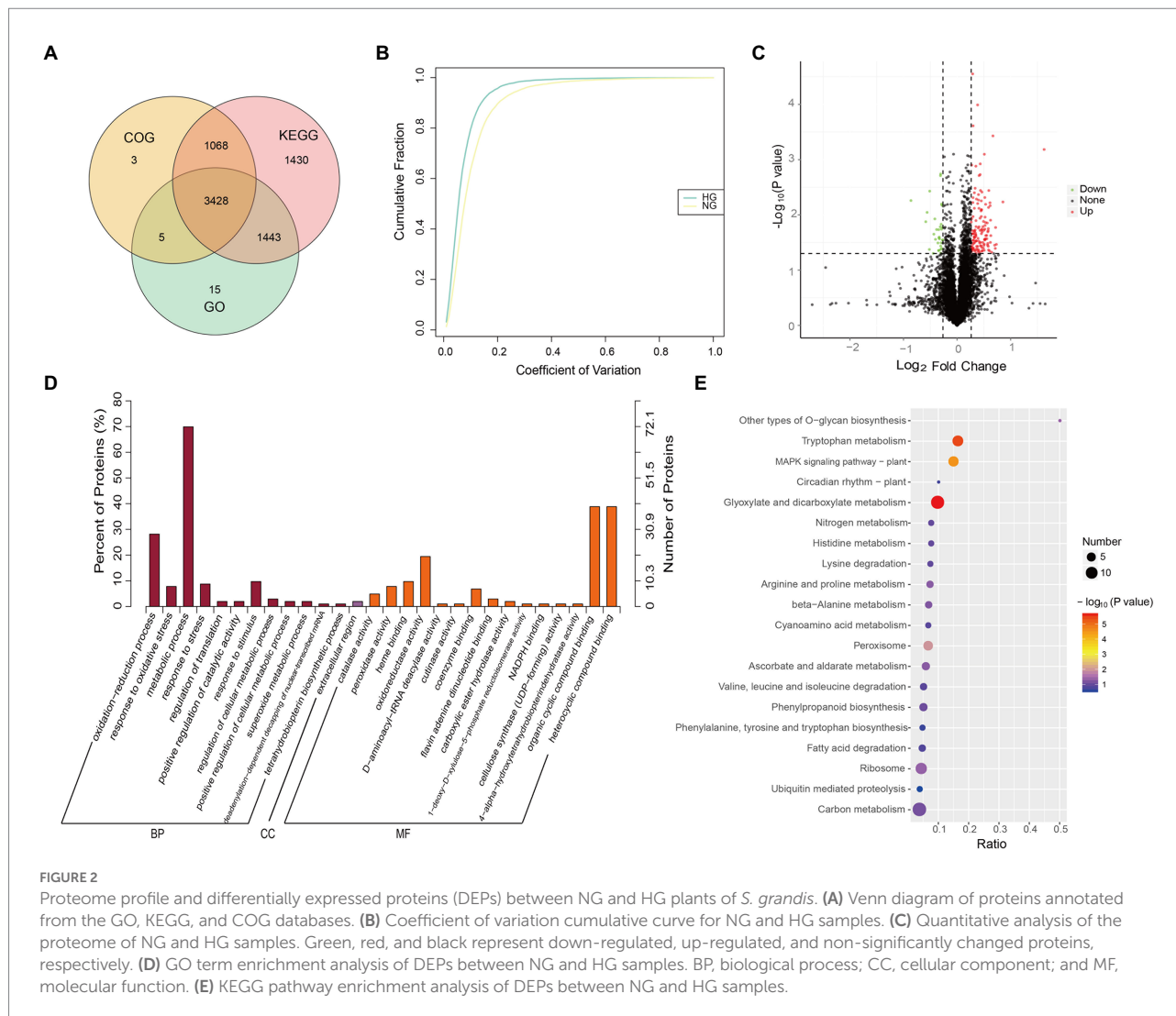
terms associated with the biological process category were oxidation–reduction process, response to oxidative stress, metabolic process, response to stress, and regulation of translation. Only one enriched term, extracellular region, was associated with the cellular component category. The KEGG pathway analysis showed that the DEPs were enriched with 36 pathways (Figure 2E; Supplementary Table S4). It was noteworthy that glyoxylate and dicarboxylate metabolism, tryptophan metabolism, MAPK signaling pathway–plant, peroxisome, other types of O-glycan biosynthesis, and ribosome pathway were significantly enriched ($p \leq 0.05$).

Widely targeted metabolic profile analysis of *Stipa grandis*

To investigate the impact of heavy grazing on metabolic changes in *S. grandis*, the metabolome was detected in leaves from HG and NG samples of *S. grandis* by LC–MS/MS analysis. In total, 717 metabolites were identified (Supplementary Table S5). The metabolites were assigned to 32 types (Figure 3A). The five most abundant metabolite types were organic acids (10.32%), flavones (9.76%), amino acid derivatives (8.79%), nucleotides and derivatives (7.81%), and flavone C-glycosides (5.72%). The PCA revealed a clear separation between HG and NG plants (Figure 3B). Similarly, the heatmap cluster analysis clearly divided the six samples into two groups (Figure 3C). In addition, the Pearson's correlation analysis showed that the intragroup samples were significantly correlated (Supplementary Figure S4).

A total of 101 metabolites differed significantly between the HG and NG groups (Figure 4A). The metabolites were classified into 21 categories, and comprised 78 upregulated and 23 downregulated metabolites (Table 1). The top 20 DAMs were mainly associated with flavones, flavone C-glycosides, quinate and its derivatives, catechin derivatives, carbohydrates, benzoic acid derivatives, organic acids, indole derivatives, hydroxycinnamoyl





derivatives, amino acid derivatives, alcohols and polyols, and phenolamides (Supplementary Figure S5).

Based on KEGG pathway classification, the DAMs were involved in 64 pathways (Supplementary Table S6). The ten most enriched metabolic pathways were (in decreasing order) flavone and flavonol biosynthesis, tryptophan (Trp) metabolism, phenylpropanoid biosynthesis, stilbenoid, diarylheptanoid, and gingerol biosynthesis, styrene degradation, linoleic acid metabolism, renal cell carcinoma, serotonin receptor agonists/antagonists, galactose metabolism, and African trypanosomiasis (Figure 4B). Notably, the flavone and flavonol biosynthesis pathway was significantly enriched ($p < 0.05$) in the comparison of HG and NG.

KEGG pathways shared among DEGs, DEPs, and DAMs

The KEGG pathway enrichment analysis of the DEGs and DAMs showed that 26 KEGG pathways were shared among the

significantly changed metabolites and transcripts (Figure 5A). Relatively high enrichment was observed among the stilbenoid, diarylheptanoid and gingerol biosynthesis, phenylpropanoid biosynthesis, tryptophan metabolism, pyruvate metabolism, degradation of aromatic compounds, indole alkaloid biosynthesis, pentose phosphate, and flavonoid biosynthesis pathways. Combined analysis of KEGG pathway enrichment among DEGs and DEPs revealed that the top shared pathways were glyoxylate and dicarboxylate metabolism, ribosome, biosynthesis of secondary metabolites, RNA degradation, and endocytosis (Figure 5B).

Joint analysis of phenylpropanoid biosynthesis, and flavone and flavonol biosynthesis

Given that flavone and flavonol biosynthesis as well as phenylpropanoid biosynthesis were among the three most highly

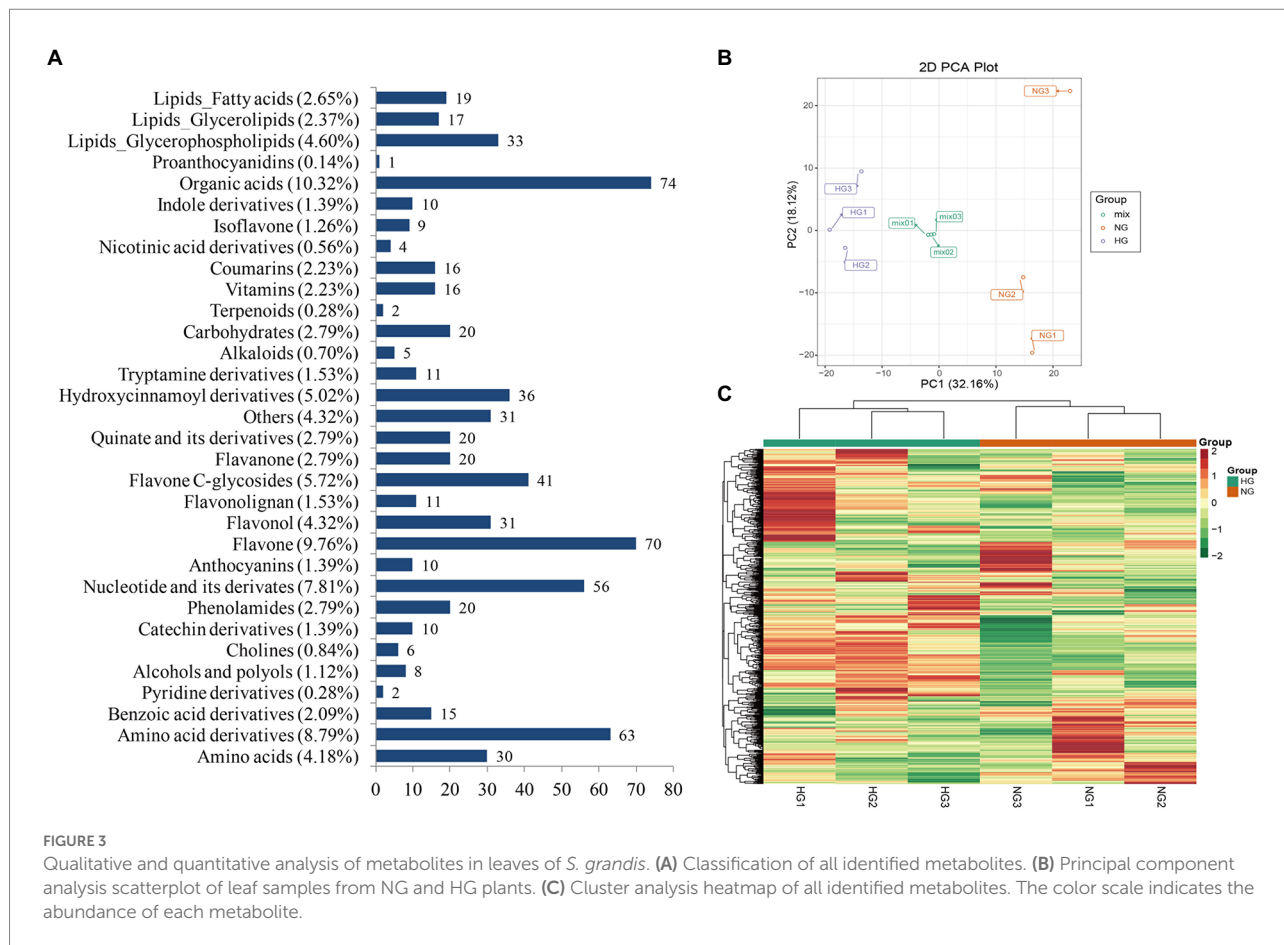


FIGURE 3 Qualitative and quantitative analysis of metabolites in leaves of *S. grandis*. (A) Classification of all identified metabolites. (B) Principal component analysis scatterplot of leaf samples from NG and HG plants. (C) Cluster analysis heatmap of all identified metabolites. The color scale indicates the abundance of each metabolite.

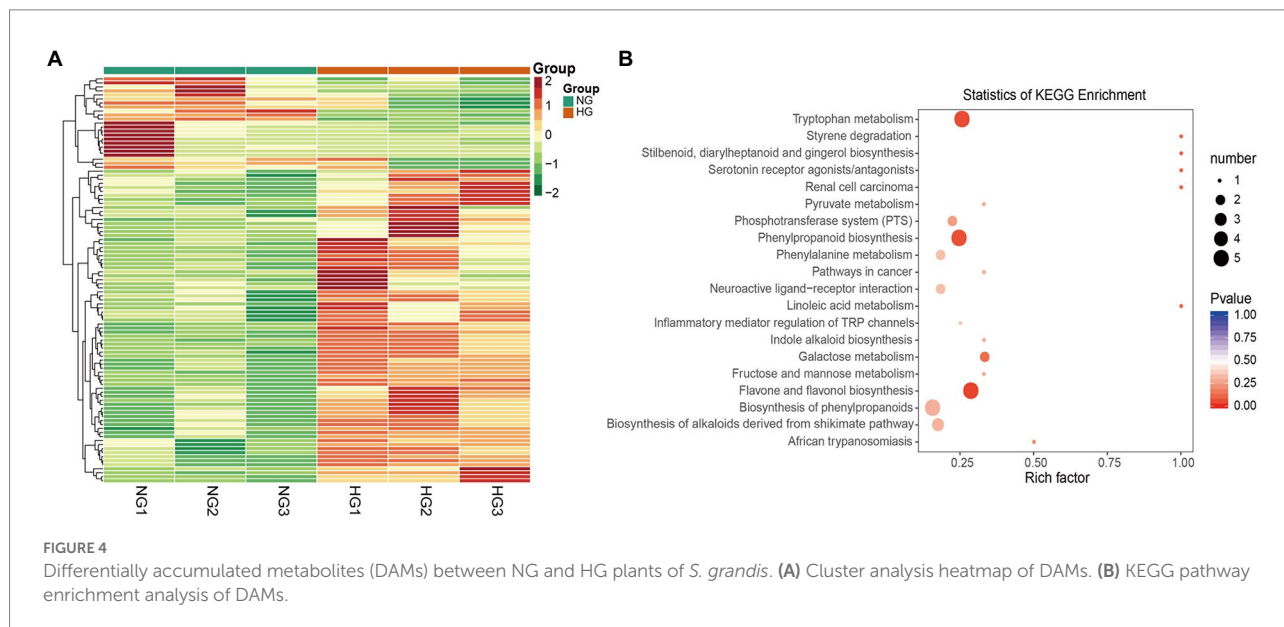


FIGURE 4 Differentially accumulated metabolites (DAMs) between NG and HG plants of *S. grandis*. (A) Cluster analysis heatmap of DAMs. (B) KEGG pathway enrichment analysis of DAMs.

enriched pathways in the metabolic profile analysis, an integrated analysis of DAMs, DEGs, and DEPs was performed (Figure 6). In the phenylpropanoid biosynthesis pathway, all of the five DAMs,

namely *p*-coumaryl alcohol, chlorogenic acid, coniferylaldehyde, coniferyl alcohol, and isoeugenol, showed decreased accumulation in HG compared with NG samples. Four proteins,

comprising two peroxidases (POD), one beta-glucosidase (BGL), and one cinnamyl-alcohol dehydrogenase (CAD), showed enhanced expression in HG compared with NG leaves. Six genes

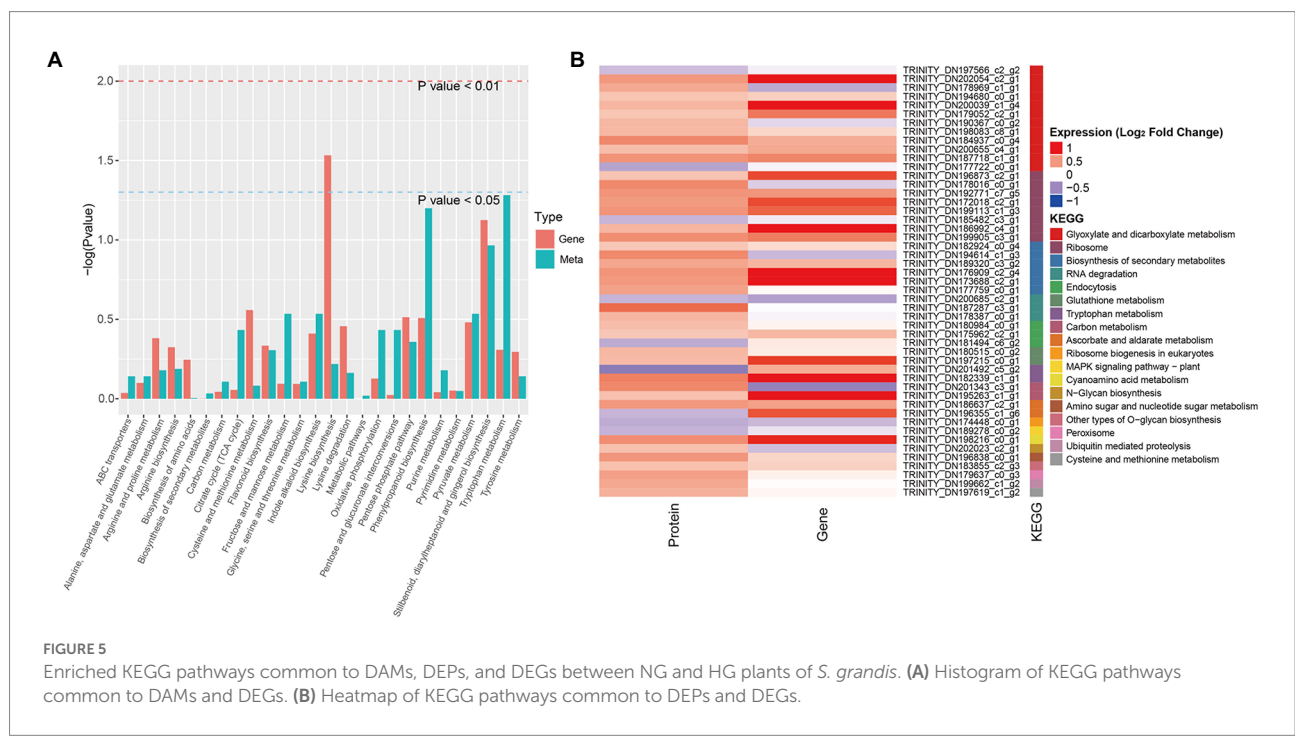
TABLE 1 Classification of significantly differentially accumulated metabolites between NG and HG plants of *S. grandis*.

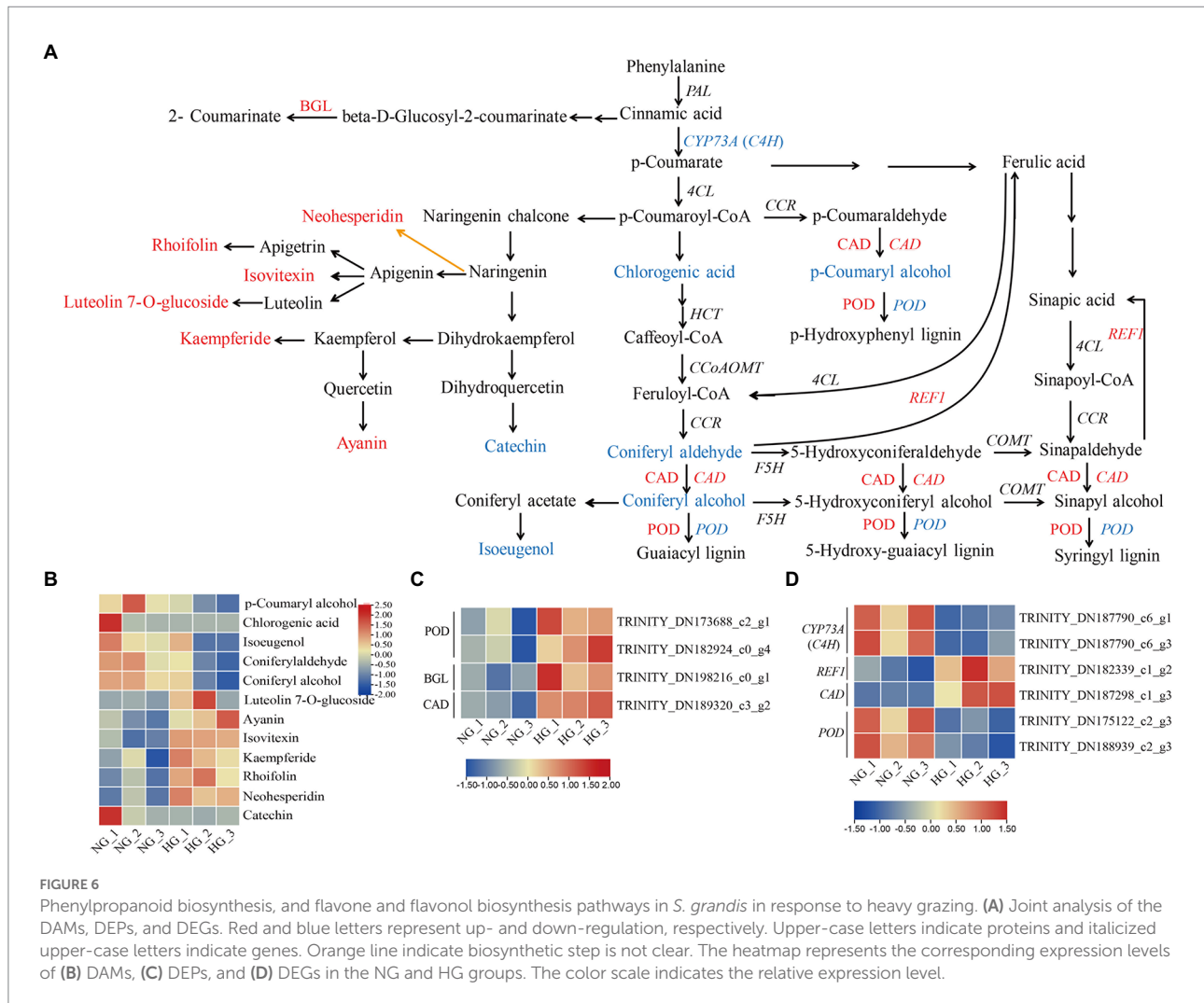
Class	Total	Up-regulation	Down-regulation
Amino acid derivatives	8	7	1
Benzoic acid derivatives	3	2	1
Alcohols and polyols	3	3	0
Catechin derivatives	2	1	1
Phenolamides	3	3	0
Nucleotide and its derivates	2	0	2
Anthocyanins	1	1	0
Flavone	22	22	0
Flavonol	6	6	0
Flavone C-glycosides	17	17	0
Flavanone	2	2	0
Quinate and its derivatives	4	0	4
Others	2	0	2
Hydroxycinnamoyl derivatives	4	0	4
Tryptamine derivatives	4	4	0
Carbohydrates	3	1	2
Indole derivatives	1	1	0
Organic acids	5	1	4
Lipids_Glycerophospholipids	5	3	2
Lipids_Glycerolipids	1	1	0
Lipids_Fatty acids	3	3	0

were differentially expressed in HG compared with the NG group, among which two *trans*-cinnamate 4-monooxygenase-encoding genes (*CYP73A*) and two POD-encoding genes were down-regulated, and one CAD-encoding gene and one cinnamyl-alcohol dehydrogenase-encoding gene (*REF1*) were up-regulated. In the flavone and flavonol biosynthesis pathway, five metabolites, namely luteolin 7-*O*-glucoside, ayanin, isovitexin, kaempferide, and rhoifolin, showed differential accumulation patterns between the HG and NG groups, with higher accumulation observed in HG than in NG samples. However, no enrichment of significant DEGs or DEPs was observed. In addition, two DAMs (neohesperidin and catechin) that were mapped to the flavonoid biosynthesis pathway showed altered accumulation in HG samples. WGCNA was performed to identify potential genes co-expression with these DAMs. The *CAD* and *REF1* were distributed to module of yellow, and negatively correlated with DAMs of phenylpropanoid biosynthesis; while *CYP73As* and *PODs* were distributed to module grey60, and positively correlated with DAMs of phenylpropanoid biosynthesis (Supplementary Figure S6).

Joint analysis of Trp metabolism

To evaluate the impact of heavy grazing on Trp metabolism, an integrated analysis of DAMs, DEPs, and DEGs associated with auxin biosynthesis was conducted (Figure 7). All five enriched metabolites involved in Trp metabolism were more highly accumulated in HG compared with NG samples, among which tryptamine (TAM), *N*-hydroxytryptamine, and





indole-3-acetonitrile (IAN) are involved in Trp-dependent indole-3-acetic acid (IAA) biosynthesis. Three DEPs were associated with IAA biosynthesis, of which two aldehyde dehydrogenase (ALDH) family 2 proteins were up-regulated, and one amidase (AMI), which is involved in the conversion of indole-3-acetamide (IAM) into active IAA, was down-regulated in HG compared with NG samples. Three DEGs associated with *ALDH* genes were up-regulated in HG compared with NG samples. WGCNA analysis showed that one and two *ALDHs* distributed to yellow and green modules, respectively, and positively correlated with the DAMs of Trp metabolism (Supplementary Figure S7).

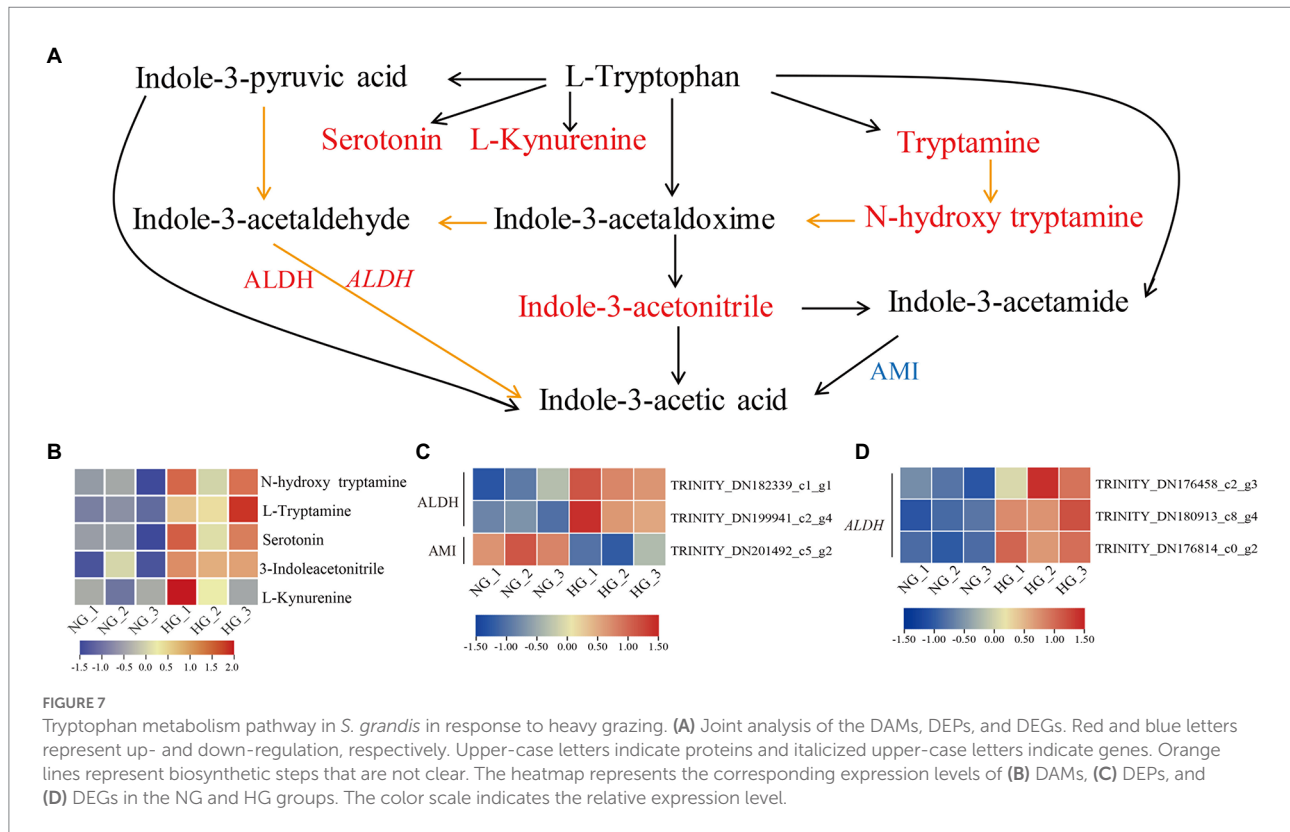
Discussion

Grazing is the most widespread and important land use in Inner Mongolia. The plant morphology, grassland productivity, and vegetation dynamics are affected by different grazing intensities (Liu et al., 2019). In this study, we investigated the

mechanism for heavy-grazing-induced plant dwarfism by conducting an integrated analysis of the transcriptome, proteome, and metabolome. Based on the metabolic profile analysis, 101 metabolites were significantly differentially accumulated ($VIP \geq 1$) between the HG and NG groups. These DAMs were assigned to 64 KEGG pathways among which the three most enriched pathways were flavone and flavonol biosynthesis, tryptophan metabolism, and phenylpropanoid biosynthesis.

Phenylpropanoid biosynthesis, and flavone and flavonol biosynthesis response to heavy grazing

The phenylpropanoid pathway is among the most extensively investigated specialized metabolic pathways (Dong and Lin, 2021). It gives rise to a vast variety of aromatic metabolites (Zhang and Liu, 2015). The lignin and flavonoid pathways are two major branches among the diverse branches of phenylpropanoid metabolism derived from the general phenylpropanoid pathway



(Dong and Lin, 2021). In which, phenylalanine is catalyzed by phenylalanine ammonia lyase to form *trans*-cinnamic acid, which is hydroxylated by cinnamic acid 4-hydroxylase (C4H) to generate *p*-coumaric acid. In turn, *p*-coumaric acid is converted into *p*-coumaroyl-CoA catalyzed by 4-coumarate-CoA ligase (4CL; Dong and Lin, 2021).

Lignin, primarily a component of secondarily thickened cell walls, is essential for mechanical support during plant growth, facilitates the transportation of water and nutrients, and plays roles in plant resistance to pathogen attack (Boerjan et al., 2003). Lignin is derived mainly from three monolignols, namely *p*-coumaryl (M1_H), coniferyl (M1_G), and sinapyl (M1_S) alcohols, which are used to produce the three basic units of lignin, *p*-hydroxyphenyl (H), guaiacyl (G), and syringyl (S), respectively (Boerjan et al., 2003; Dong and Lin, 2021). Alteration of monolignol metabolism strongly impacts on plant growth (Meents et al., 2018). However, the mechanism of dwarfism caused by suppression of monolignol biosynthesis is not completely elucidated, but several factors may contribute, such as water transport disruption, lack of cell proliferation or expansion resulting from failed synthesis of a phenylpropanoid-derived compound, or accumulation of a toxic pathway intermediate (Bonawitz and Chapple, 2010). In the present study, four of the five DAMs enriched in phenylpropanoid biosynthesis that were decreased in abundance in HG were involved in lignin biosynthesis, namely chlorogenic acid, coniferylaldehyde, and the monolignols coniferyl alcohol and *p*-coumaryl alcohol. Inconsistent with this finding, three enzymes were more highly

accumulated in HG compared with NG. One of these enzymes was CAD, which functions in the final step of monolignol biosynthesis and is responsible for catalyzing the cinnamaldehydes to the corresponding alcohols, namely *p*-coumaryl alcohol, coniferyl alcohol, coniferyl alcohol, 5H coniferyl alcohol, and sinapyl alcohol (Boerjan et al., 2003; Dong and Lin, 2021). The other two enzymes were PODs, which are involved in the dehydrogenative polymerization of monolignols to form lignin (Fraser and Chapple, 2011). One CAD-encoding gene was up-regulated and two POD-encoding genes were downregulated. The inconsistent expression patterns of POD proteins and *POD* genes may result from the lower correlation between transcript and protein level due to post-transcriptional and post-translational regulations (Kumar et al., 2016; Xu et al., 2021). Alternatively, because these belong to a different member of POD family that may play different roles in lignin biosynthesis. C4H is a unique member of CYP73A, termed as CYP73A5 in *Arabidopsis thaliana* (Mizutani et al., 1997; Fraser and Chapple, 2011). Mutant of *C4H* displayed a dwarf phenotype in *A. thaliana* (Schillmiller et al., 2009). In the present study, down-regulated expression of two *C4H* members, i.e. the CYP73A genes, in HG compared with NG, may be positively related to the heavy-grazing-induced dwarfism of *S. grandis*. Taken together, these results indicated that monolignol biosynthesis was inactivated in the heavy-grazing-induced dwarfism of *S. grandis*, and decreased production of monolignols may be associated with the plant morphological phenotype and reduction of lignin-mediated defense responses. But the regulatory mechanism of reduced monolignol

biosynthesis associated with the dwarfism of *S. grandis* remains unclear. Additionally, the activated expression of proteins or genes in HG may be associated with restored promotion of growth following the exclusion of grazing after the spring regreening stage. Further research on the molecular regulation of monolignol biosynthesis activity to adapt to heavy grazing is necessary.

Flavonoids, a major class of phenolic compounds, possess a basic C6–C3–C6 skeleton and are divided into numerous subgroups, such as flavanones, flavanols, flavones, and flavonols (Nakayama et al., 2019; Nabavi et al., 2020). Flavonoids perform a wide range of roles in plant development and environmental adaptation (Peer and Murphy, 2007; Thompson et al., 2010; Hichri et al., 2011). In particular, flavonoid biosynthesis is induced by oxidative stress (Nabavi et al., 2020), and flavonoids act as antioxidants to decrease oxidative damage triggered by reactive oxygen species under exposure to stresses (Nakabayashi and Saito, 2015; Dong and Lin, 2021). In the present study, all five DAMs involved in flavone and flavonol biosynthesis were more highly accumulated in the HG group than in NG samples. Except for ayanin, which has antimicrobial activity (French et al., 1991), the other four metabolites, namely luteolin 7-*O*-glucoside, isovitexin, kaempferide, and rhoifolin, exhibit antioxidant capabilities (Picerno et al., 2003; Eldahshan and Azab, 2012; Bian et al., 2013; Lama-Muñoz et al., 2019). This finding indicated that heavy-grazing-induced dwarfism may enhance tolerance to environmental stresses and might be mediated by flavonoid compounds through decreased oxidative damage. However, little is known about the underlying regulatory mechanism. Grazing caused multi-stress, involved in trampling/wounding, defoliation, saliva deposition, and manure deposition (Chen et al., 2009). Over or heavy grazing resulted in grassland degradation, including but not limited to reduced vegetation coverage and species diversity, declined plant growth, decreased soil coverage and water conservation, as well as changed soil microbial structure (Han et al., 2008; Yang et al., 2016). Whether these factors contribute to the changed accumulation pattern of flavonoids in dwarf plants, and which is the driving factor, is worth further confirmation by conducting the single or cross-stress experiments in *S. grandis*.

Trp metabolism response to heavy grazing

The most abundant and intensively studied endogenous auxin is IAA, which is essential for plant growth and development (Yue et al., 2014; Kasahara, 2016). In the Trp metabolism pathway, Trp is a precursor of auxin and various secondary metabolites (Maeda and Dudareva, 2012). The IAA is mainly synthesized by Trp-dependent and Trp-independent pathways (Mano and Nemoto, 2012). In the Trp-dependent pathway, IAA can be derived from the following pathways: Trp, IAM and IAA in the IAM pathway; Trp, indole-3-pyruvic acid (IPA), indole-3-acetaldehyde (IAAld) and IAA in the IPA

pathway; Trp, indole-3-acetaldoxime (IAOx), IAN or IAAlD, and IAA in the IAOx pathway; and Trp, TAM, *N*-hydroxytryptamine, IAOx, IAAlD, and IAA in the TAM pathway (Woodward and Bartel, 2005; Mano and Nemoto, 2012). In the present study, TAM, *N*-hydroxytryptamine, and IAN showed elevated accumulation in heavy-grazing-induced dwarfed plants compared with NG plants, but the IAA content showed no obvious difference between the two groups. In addition, the expression level of AMI1, which converts IAM to IAA, was decreased in dwarfed plants. Fine-tuning of cellular auxin contents is important for plant survival (Casanova-Saez and Voss, 2019). We hypothesized that auxin contents are fine-tuned in heavily grazed plants and may play important roles in the regulation of plant development and responses to environmental stresses. In further studies, it will be important to explore the cross-talk of IAA with other phytohormones in the regulation of heavy grazing response.

Data availability statement

The mass spectrometry proteomics data presented in the study are deposited in the ProteomeXchange Consortium (<http://proteomecentral.proteomexchange.org>) via the iProX partner repository, accession number PXD035914. The transcriptomic data presented in the study are deposited in the NCBI Sequence Read Archive (SRA) repository, accession number PRJNA867365.

Author contributions

DW and YD conceived and designed the experiments. DW and YW performed the experiments. DW, YW, TZ, and RW analyzed the data. DW drafted the manuscript. All authors contributed to the article and approved the submitted version.

Funding

This research was funded by the Natural Science Foundation of Inner Mongolia Autonomous Region (2020ZD06 and 2022LHMS03007), Key technology Project of Science and Technology Plan in Inner Mongolia Autonomous (2019GG009), Major special projects of science and technology in Inner Mongolia Autonomous Region (2019ZD008), and the Central Public-interest Scientific Institution Basal Research Fund (1610332020004).

Acknowledgments

We thank Robert McKenzie, PhD, from Liwen Bianji (Edanz) (www.liwenbianji.cn) for editing the English text of a draft of this manuscript.

Conflict of interest

The authors declare that the research was conducted in the absence of any commercial or financial relationships that could be construed as a potential conflict of interest.

Publisher's note

All claims expressed in this article are solely those of the authors and do not necessarily represent those of their affiliated

organizations, or those of the publisher, the editors and the reviewers. Any product that may be evaluated in this article, or claim that may be made by its manufacturer, is not guaranteed or endorsed by the publisher.

Supplementary material

The Supplementary material for this article can be found online at: <https://www.frontiersin.org/articles/10.3389/fpls.2022.995074/full#supplementary-material>

References

- Balcke, G. U., Bennewitz, S., Bergau, N., Athmer, B., Henning, A., Majovsky, P., et al. (2017). Multi-Omics of tomato glandular Trichomes reveals distinct features of central carbon metabolism supporting high productivity of specialized metabolites. *Plant Cell* 29, 960–983. doi: 10.1105/tpc.17.00060
- Bian, Q. Y., Wang, S. Y., Xu, L. J., Chan, C. O., Mok, D. K., and Chen, S. B. (2013). Two new antioxidant diarylheptanoids from the fruits of *Alpinia oxyphylla*. *J. Asian Nat. Prod. Res.* 15, 1094–1099. doi: 10.1080/10286020.2013.816297
- Boerjan, W., Ralph, J., and Baucher, M. (2003). Lignin biosynthesis. *Annu. Rev. Plant Biol.* 54, 519–546. doi: 10.1146/annurev.arplant.54.031902.134938
- Bonawitz, N. D., and Chapple, C. (2010). The genetics of lignin biosynthesis: connecting genotype to phenotype. *Annu. Rev. Genet.* 44, 337–363. doi: 10.1146/annurev-genet-102209-163508
- Bradford, M. M. (1976). A rapid and sensitive method for the quantitation of microgram quantities of protein utilizing the principle of protein-dye binding. *Anal. Biochem.* 72, 248–254. doi: 10.1016/0003-2697(76)90527-3
- Casanova-Saez, R., and Voss, U. (2019). Auxin metabolism controls developmental decisions in land plants. *Trends Plant Sci.* 24, 741–754. doi: 10.1016/j.tplants.2019.05.006
- Chauffour, F., Bailly, M., Perreau, F., Cueff, G., Suzuki, H., Collet, B., et al. (2019). Multi-omics analysis reveals sequential roles for ABA during seed maturation. *Plant Physiol.* 180, 1198–1218. doi: 10.1104/pp.19.00338
- Chen, W., Gong, L., Guo, Z., Wang, W., Zhang, H., Liu, X., et al. (2013). A novel integrated method for large-scale detection, identification, and quantification of widely targeted metabolites: application in the study of rice metabolomics. *Mol. Plant* 6, 1769–1780. doi: 10.1093/mp/sst080
- Chen, J., Han, G., Shang, C., Li, J., Zhang, H., Liu, F., et al. (2015). Proteomic analyses reveal differences in cold acclimation mechanisms in freezing-tolerant and freezing-sensitive cultivars of alfalfa. *Front. Plant Sci.* 6:105. doi: 10.3389/fpls.2015.00105
- Chen, J., Hu, X., Shi, T., Yin, H., Sun, D., Hao, Y., et al. (2020). Metabolite-based genome-wide association study enables dissection of the flavonoid decoration pathway of wheat kernels. *Plant Biotechnol. J.* 18, 1722–1735. doi: 10.1111/pbi.13335
- Chen, S., Li, X. Q., Zhao, A., Wang, L., Li, X., Shi, Q., et al. (2009). Genes and pathways induced in early response to defoliation in rice seedlings. *Curr. Issues Mol. Biol.* 11, 81–100. doi: 10.21775/cimb.011.081
- Chen, C., Zhou, G., Chen, J., Liu, X., Lu, X., Chen, H., et al. (2021). Integrated metabolome and transcriptome analysis unveils novel pathway involved in the formation of yellow Peel in cucumber. *Int. J. Mol. Sci.* 22:1494. doi: 10.3390/ijms22031494
- Decourcelle, M., Perez-Fons, L., Baulande, S., Steiger, S., Couvelard, L., Hem, S., et al. (2015). Combined transcript, proteome, and metabolite analysis of transgenic maize seeds engineered for enhanced carotenoid synthesis reveals pleiotropic effects in core metabolism. *J. Exp. Bot.* 66, 3141–3150. doi: 10.1093/jxb/erv120
- Dong, N. Q., and Lin, H. X. (2021). Contribution of phenylpropanoid metabolism to plant development and plant-environment interactions. *J. Integr. Plant Biol.* 63, 180–209. doi: 10.1111/jipb.13054
- Eldahshan, O. A., and Azab, S. S. (2012). Anti-inflammatory effect of Apigenin-7-neohesperidoside (Rhoifolin) in Carrageenin-induced rat Oedema model. *J. Appl. Pharm. Sci.* 2, 74–79. doi: 10.7324/JAPS.2012.2811
- Fraga, C. G., Clowers, B. H., Moore, R. J., and Zink, E. M. (2010). Signature-discovery approach for sample matching of a nerve-agent precursor using liquid chromatography-mass spectrometry, XCMS, and Chemometrics. *Anal. Chem.* 82, 4165–4173. doi: 10.1021/ac1003568
- Fraser, C. M., and Chapple, C. (2011). The phenylpropanoid pathway in *Arabidopsis*. *Arabidopsis Book*. 9:e0152. doi: 10.1199/tab.0152
- French, C. J., Elder, M., Leggett, F., Ibrahim, R. K., and Neil Towers, G. H. (1991). Flavonoids inhibit infectivity of tobacco mosaic virus. *Can. J. Plant Pathol.* 13, 1–6. doi: 10.1080/07060669109500959
- Gao, S. B., Mo, L. D., Zhang, L. H., Zhang, J. L., Wu, J. B., Wang, J. L., et al. (2018b). Phenotypic plasticity vs. local adaptation in quantitative traits differences of *Stipa grandis* in semi-arid steppe. *China Sci. Rep.* 8:3148. doi: 10.1038/s41598-018-21557-w
- Gao, S., Zheng, Z., Wang, Y., Liu, L., Zhao, N., and Gao, Y. (2018a). Drought and grazing drive the retrogressive succession by changing the plant-plant interaction of the main species in Inner Mongolia steppe. *Ecol. Evol.* 8, 11954–11963. doi: 10.1002/ece3.4652
- Grabherr, M. G., Haas, B. J., Yassour, M., Levin, J. Z., Thompson, D. A., Amit, I., et al. (2011). Full-length transcriptome assembly from RNA-Seq data without a reference genome. *Nat. Biotechnol.* 29, 644–652. doi: 10.1038/nbt.1883
- Guo, Q., Li, X., Niu, L., Jameson, P. E., and Zhou, W. (2021). Transcription-associated metabolomic adjustments in maize occur during combined drought and cold stress. *Plant Physiol.* 186, 677–695. doi: 10.1093/plphys/kiab050
- Han, J. G., Zhang, Y. J., Wang, C. J., Bai, W. M., Wang, Y. R., Han, G. D., et al. (2008). Rangeland degradation and restoration management in China. *Rangel. J.* 30, 233–239. doi: 10.1071/RJ08009
- Hichri, I., Barrieu, F., Bogs, J., Kappel, C., Delrot, S., and Lauvergeat, V. (2011). Recent advances in the transcriptional regulation of the flavonoid biosynthetic pathway. *J. Exp. Bot.* 62, 2465–2483. doi: 10.1093/jxb/Erq442
- Jiang, Z., Jin, F., Shan, X., and Li, Y. (2019). iTRAQ-based proteomic analysis reveals several strategies to cope with drought stress in maize seedlings. *Int. J. Mol. Sci.* 20:5956. doi: 10.3390/ijms20235956
- Job, D., Haynes, P. A., and Zivy, M. (2011). Plant proteomics. *Proteomics* 11, 1557–1558. doi: 10.1002/pmic.201190035
- Kasahara, H. (2016). Current aspects of auxin biosynthesis in plants. *Biosci. Biotechnol. Biochem.* 80, 34–42. doi: 10.1080/09168451.2015.1086259
- Kumar, D., Bansal, G., Narang, A., Basak, T., Abbas, T., and Dash, D. (2016). Integrating transcriptome and proteome profiling: strategies and applications. *Proteomics* 16, 2533–2544. doi: 10.1002/pmic.201600140
- Lama-Muñoz, A., Del Mar Contreras, M., Espinola, F., Moya, M., De Torres, A., Romero, I., et al. (2019). Extraction of oleuropein and luteolin-7-O-glucoside from olive leaves: optimization of technique and operating conditions. *Food Chem.* 293, 161–168. doi: 10.1016/j.foodchem.2019.04.075
- Li, X., Bi, X., An, M., Xia, Z., and Wu, Y. (2020). iTRAQ-based proteomic analysis of watermelon fruits in response to cucumber green mottle mosaic virus infection. *Int. J. Mol. Sci.* 21:2541. doi: 10.3390/ijms21072541
- Li, S. P., Deng, B. L., Tian, S., Guo, M. X., Liu, H. X., and Zhao, X. S. (2021a). Metabolic and transcriptomic analyses reveal different metabolite biosynthesis profiles between leaf buds and mature leaves in *Ziziphus jujuba* mill. *Food Chem.* 347:129005. doi: 10.1016/j.foodchem.2021.129005
- Li, X., Huang, Q., Mi, X., Bai, Y., Zhang, M., and Li, X. (2018). Grazing every month minimizes size but boosts photosynthesis in *Stipa grandis* in the steppe of Inner Mongolia. *China J. Arid Land.* 10, 601–611. doi: 10.1007/s40333-018-0011-4
- Li, X. L., Liu, Z. Y., Wang, Z., Wu, X. H., Li, X. L., Hu, J., et al. (2015). Pathways of *Leymus chinensis* individual aboveground biomass decline in natural semiarid grassland induced by overgrazing: a study at the plant functional trait scale. *PLoS One* 10:e0124443. doi: 10.1371/journal.pone.0124443
- Li, Q., and Song, J. (2019). Analysis of widely targeted metabolites of the euhalophyte *Suaeda salsa* under saline conditions provides new insights into salt tolerance and nutritional value in halophytic species. *BMC Plant Biol.* 19:388. doi: 10.1186/s12870-019-2006-5

- Li, W., Wen, L., Chen, Z., Zhang, Z., Pang, X., Deng, Z., et al. (2021b). Study on metabolic variation in whole grains of four proso millet varieties reveals metabolites important for antioxidant properties and quality traits. *Food Chem.* 357:129791. doi: 10.1016/j.foodchem.2021.129791
- Liu, M., Gong, J., Yang, B., Ding, Y., Zhang, Z., Wang, B., et al. (2019). Differences in the photosynthetic and physiological responses of *Leymus chinensis* to different levels of grazing intensity. *BMC Plant Biol.* 19:558. doi: 10.1186/s12870-019-2184-1
- Liu, B., Zhang, N., Zhao, S., Chang, J., Wang, Z., Zhang, G., et al. (2015). Proteomic changes during tuber dormancy release process revealed by iTRAQ quantitative proteomics in potato. *Plant Physiol. Biochem.* 86, 181–190. doi: 10.1016/j.plaphy.2014.12.003
- Love, M. I., Huber, W., and Anders, S. (2014). Moderated estimation of fold change and dispersion for RNA-seq data with DESeq2. *Genome Biol.* 15:550. doi: 10.1186/s13059-014-0550-8
- Lv, J., Zheng, T., Song, Z., Pervais, T., Dong, T., Zhang, Y., et al. (2021). Strawberry proteome responses to controlled hot and cold stress partly mimic post-harvest storage temperature effects on fruit quality. *Front. Nutr.* 8:812666. doi: 10.3389/fnut.2021.812666
- Maeda, H., and Dudareva, N. (2012). The Shikimate pathway and aromatic amino acid biosynthesis in plants. *Annu. Rev. Plant Biol.* 63, 73–105. doi: 10.1146/annurev-arplant-042811-105439
- Mann, M., Kulak, N. A., Nagaraj, N., and Cox, J. (2013). The coming age of complete, accurate, and ubiquitous proteomes. *Mol. Cell* 49, 583–590. doi: 10.1016/j.molcel.2013.01.029
- Mano, Y., and Nemoto, K. (2012). The pathway of auxin biosynthesis in plants. *J. Exp. Bot.* 63, 2853–2872. doi: 10.1093/jxb/ers091
- Meents, M. J., Watanabe, Y., and Samuels, A. L. (2018). The cell biology of secondary cell wall biosynthesis. *Ann. Bot.* 121, 1107–1125. doi: 10.1093/aob/mcy005
- Mizutani, M., Ohta, D., and Sato, R. (1997). Isolation of a cDNA and a genomic clone encoding cinnamate 4-hydroxylase from *Arabidopsis* and its expression manner in planta. *Plant Physiol.* 113, 755–763. doi: 10.1104/pp.113.3.755
- Nabavi, S. M., Samec, D., Tomczyk, M., Milella, L., Russo, D., Habtemariam, S., et al. (2020). Flavonoid biosynthetic pathways in plants: versatile targets for metabolic engineering. *Biotechnol. Adv.* 38:107316. doi: 10.1016/j.biotechadv.2018.11.005
- Nakabayashi, R., and Saito, K. (2015). Integrated metabolomics for abiotic stress responses in plants. *Curr. Opin. Plant Biol.* 24, 10–16. doi: 10.1016/j.cpb.2015.01.003
- Nakayama, T., Takahashi, S., and Waki, T. (2019). Formation of flavonoid Metabolons: functional significance of protein-protein interactions and impact on flavonoid Chemodiversity. *Front. Plant Sci.* 10:821. doi: 10.3389/fpls.2019.00821
- Pandey, A., and Mann, M. (2000). Proteomics to study genes and genomes. *Nature* 405, 837–846. doi: 10.1038/35015709
- Peer, W. A., and Murphy, A. S. (2007). Flavonoids and auxin transport: modulators or regulators? *Trends Plant Sci.* 12, 556–563. doi: 10.1016/j.tplants.2007.10.003
- Picerno, P., Mencherini, T., Lauro, M. R., Barbato, F., and Aquino, R. (2003). Phenolic constituents and antioxidant properties of *Xanthosoma violaceum* leaves. *J. Agric. Food Chem.* 51, 6423–6428. doi: 10.1021/jf030284h
- Qin, X., Yin, Y., Zhao, J., An, W., Fan, Y., Liang, X., et al. (2022). Metabolomic and transcriptomic analysis of *Lycium chinense* and *L. ruthenicum* under salinity stress. *BMC Plant Biol.* 22:8. doi: 10.1186/s12870-021-03375-x
- Ren, W., Hou, X., Wu, Z., Kong, L., Guo, H., Hu, N., et al. (2018a). De novo transcriptomic profiling of the clonal *Leymus chinensis* response to long-term overgrazing-induced memory. *Sci. Rep.* 8:17912. doi: 10.1038/s41598-018-35605-y
- Ren, W., Hu, N., Hou, X., Zhang, J., Guo, H., Liu, Z., et al. (2017). Long-term overgrazing-induced memory decreases photosynthesis of clonal offspring in a perennial grassland plant. *Front. Plant Sci.* 8:419. doi: 10.3389/fpls.2017.00419
- Ren, W., Xie, J., Hou, X., Li, X., Guo, H., Hu, N., et al. (2018b). Potential molecular mechanisms of overgrazing-induced dwarfism in sheepgrass (*Leymus chinensis*) analyzed using proteomic data. *BMC Plant Biol.* 18:81. doi: 10.1186/s12870-018-1304-7
- Saito, K., and Matsuda, F. (2010). Metabolomics for functional genomics, systems biology, and biotechnology. *Annu. Rev. Plant Biol.* 61, 463–489. doi: 10.1146/annurev-arplant.043008.092035
- Schillmiller, A. L., Stout, J., Weng, J. K., Humphreys, J., Ruegger, M. O., and Chapple, C. (2009). Mutations in the cinnamate 4-hydroxylase gene impact metabolism, growth and development in *Arabidopsis*. *Plant J.* 60, 771–782. doi: 10.1111/j.1365-313X.2009.03996.x
- Shi, T. T., Zhu, A. N., Jia, J. Q., Hu, X., Chen, J., Liu, W., et al. (2020). Metabolomics analysis and metabolite-agronomic trait associations using kernels of wheat (*Triticum aestivum*) recombinant inbred lines. *Plant J.* 103, 279–292. doi: 10.1111/tpj.14727
- Thompson, E. P., Wilkins, C., Demidchik, V., Davies, J. M., and Glover, B. J. (2010). An *Arabidopsis* flavonoid transporter is required for anther dehiscence and pollen development. *J. Exp. Bot.* 61, 439–451. doi: 10.1093/jxb/erp312
- Varet, H., Brillet-Gueguen, L., Coppee, J. Y., and Dillies, M. A. (2016). SARTools: a DESeq2 and EdgeR-based R pipeline for comprehensive differential analysis of RNA-Seq data. *PLoS One* 11:e0157022. doi: 10.1371/journal.pone.0157022
- Wan, D. L., Wan, Y. Q., Hou, X. Y., Ren, W. B., Ding, Y., and Sa, R. L. (2015). De novo assembly and Transcriptomic profiling of the grazing response in *Stipa grandis*. *PLoS One* 10:e0122641. doi: 10.1371/journal.pone.0122641
- Wang, F., Chen, N., and Shen, S. (2021a). iTRAQ-based quantitative proteomics analysis reveals the mechanism of Golden-yellow leaf mutant in hybrid paper mulberry. *Int. J. Mol. Sci.* 23:127. doi: 10.3390/ijms23010127
- Wang, F., Ge, S. F., Xu, X. X., Xing, Y., Du, X., Zhang, X., et al. (2021b). Multiomics analysis reveals new insights into the apple fruit quality decline under high nitrogen conditions. *J. Agric. Food Chem.* 69, 5559–5572. doi: 10.1021/acs.jafc.1c01548
- Woodward, A. W., and Bartel, B. (2005). Auxin: regulation, action, and interaction. *Ann. Bot.* 95, 707–735. doi: 10.1093/aob/mci083
- Wu, J. B., Gao, Y. B., Bao, X. Y., Gao, H., Jia, M. Q., Li, J., et al. (2010a). Genetic diversity of *Stipa grandis* P Smirn populations across the species range in the Inner Mongolia plateau of China. *Biochem. Syst. Ecol.* 38, 471–477. doi: 10.1016/j.bse.2010.04.008
- Wu, J. B., Gao, Y. B., Bao, X. Y., Gao, H., Jia, M. Q., Li, J., et al. (2010b). Genetic variation among *Stipa grandis* P Smirn populations with different durations of fencing in the inner Mongolian steppe. *Rangel. J.* 32, 427–434. doi: 10.1071/Rj09038
- Xiao, X. M., Wang, Y. F., Jiang, S., Ojima, D. S., and Bonham, C. D. (1995). Interannual variation in the climate and aboveground biomass of *Leymus-Chinese* steppe and *Stipa-Grandis* steppe in the Xilin River basin, inner-Mongolia. *China J. Arid Environ.* 31, 283–299. doi: 10.1016/S0140-1963(05)80033-3
- Xu, X., Legay, S., Sergeant, K., Zorzan, S., Leclercq, C. C., Charton, S., et al. (2021). Molecular insights into plant desiccation tolerance: transcriptomics, proteomics and targeted metabolite profiling in *Craterostigma plantagineum*. *Plant J.* 107, 377–398. doi: 10.1111/tpj.15294
- Xu, J. D., Yan, J. J., Li, W. J., Wang, Q. Y., Wang, C. X., Guo, J. X., et al. (2020). Integrative analyses of widely targeted metabolic profiling and Transcriptome data reveals molecular insight into Metabolic variations during apple (*Malus domestica*) fruit development and ripening. *Int. J. Mol. Sci.* 21:4797. doi: 10.3390/ijms211134797
- Yang, Z., Xiong, W., Xu, Y., Jiang, L., Zhu, E., Zhan, W., et al. (2016). Soil properties and species composition under different grazing intensity in an alpine meadow on the Eastern Tibetan plateau. *China Environ. Monit. Assess.* 188:678. doi: 10.1007/s10661-016-5663-y
- Yang, F., Yang, T., Liu, K., Yang, Q., Wan, Y., Wang, R., et al. (2019a). Analysis of metabolite accumulation related to pod color variation of *Caragana intermedia*. *Molecules* 24:717. doi: 10.3390/molecules24040717
- Yang, M., Yang, J., Su, L., Sun, K., Li, D., Liu, Y., et al. (2019b). Metabolic profile analysis and identification of key metabolites during rice seed germination under low-temperature stress. *Plant Sci.* 289:110282. doi: 10.1016/j.plantsci.2019.110282
- Yu, G. C., Wang, L. G., Han, Y. Y., and He, Q. Y. (2012). clusterProfiler: an R package for comparing biological themes among gene clusters. *Omic-a J. Integr. Biol.* 16, 284–287. doi: 10.1089/omi.2011.0118
- Yue, J., Hu, X., and Huang, J. (2014). Origin of plant auxin biosynthesis. *Trends Plant Sci.* 19, 764–770. doi: 10.1016/j.tplants.2014.07.004
- Zhan, Y., Wu, Q., Chen, Y., Tang, M., Sun, C., Sun, J., et al. (2019). Comparative proteomic analysis of okra (*Abelmoschus esculentus* L.) seedlings under salt stress. *BMC Genomics* 20:381. doi: 10.1186/s12864-019-5737-7
- Zhang, Z., Gong, J., Wang, B., Li, X., Ding, Y., Yang, B., et al. (2020). Regrowth strategies of *Leymus chinensis* in response to different grazing intensities. *Ecol. Appl.* 30:e02113. doi: 10.1002/eap.2113
- Zhang, Y., Li, Y., Li, W., Hu, Z., Yu, X., Tu, Y., et al. (2019). Metabolic and molecular analysis of nonuniform anthocyanin pigmentation in tomato fruit under high light. *Hortic. Res.* 6:56. doi: 10.1038/s41438-019-0138-2
- Zhang, X., and Liu, C. J. (2015). Multifaceted regulations of gateway enzyme phenylalanine ammonia-lyase in the biosynthesis of phenylpropanoids. *Mol. Plant* 8, 17–27. doi: 10.1016/j.molp.2014.11.001
- Zhang, Z., Wu, S., Stenoien, D. L., and Paša-Tolić, L. (2014). High-throughput proteomics. *Annu. Rev. Anal. Chem.* 7, 427–454. doi: 10.1146/annurev-anchem-071213-020216
- Zhao, W., Chen, S. P., Han, X. G., and Lin, G. H. (2009). Effects of long-term grazing on the morphological and functional traits of *Leymus chinensis* in the semiarid grassland of Inner Mongolia. *Ecol. Res.* 24, 99–108. doi: 10.1007/s11284-008-0486-0
- Zhao, N. X., Gao, Y. B., Wang, J. L., and Ren, A. Z. (2008). Population structure and genetic diversity of *Stipa grandis* P Smirn, a dominant species in the typical steppe of Northern China. *Biochem. Syst. Ecol.* 36, 1–10. doi: 10.1016/j.bse.2007.08.004